

The identification of physical close galaxy pairs

D.S.L. Soares

Departamento de Física, ICEx, UFMG, C.P. 702, 30123-970 Belo Horizonte, MG Brazil

dsoares@fisica.ufmg.br

ABSTRACT

A classification scheme for close pairs of galaxies is proposed. The scheme is motivated by the fact that the majority of apparent close pairs are in fact wide pairs in three-dimensional space. This is demonstrated by means of numerical simulations of random samples of binary galaxies and the scrutiny of the resulting projected and spatial separation distributions.

Observational strategies for classifying close pairs according to the scheme are suggested. As a result, physical — i.e., bound and spatially — close pairs are identified.

Subject headings: galaxies: interactions — galaxies: kinematics and dynamics — galaxies: structure

1. Introduction

The investigation of binary galaxies is jeopardized by the intrinsic lack of temporal observational tracking of the orbital parameter space because orbital periods are of the order of hundreds of million years. The alternative is the statistical study of samples of pairs relying on reasonable frequency distributions of the relevant orbital parameters. This has been done often since the pioneer work by Holmberg (1937) in the field. Besides the unknowns mentioned above there is a second major setback: binary galaxy catalogues are always *contaminated* by the so-called *optical* pairs, i.e., unphysical, unbound pairs seen in projection on the plane of sky. Earlier works, including Holmberg's, dealt with the problem by imposing restrictive selection criteria in the catalogues (e.g., Page et al. 1961, Karachentsev 1972, 1987, Turner 1976). Consequently the projected linear separations of pairs in these catalogues are typically 50 kpc. If one intends to study the distribution of galaxy mass to larger spatial extents such samples are clearly not adequate. A large sample of wide pairs is important in the determination of the size of dark halos, believed to exist within and around the visible parts of galaxies. Later attempts have been made in this direction (van Moorsel 1982,

Schweizer 1987, Soares 1989, Charlton & Salpeter 1991, Chengalur et al. 1993, Nordgren et al. 1998) with the addition of wide pairs with separations as large as 1 Mpc, and even more. The contamination by optical pairs remained a fundamental issue in all of these works.

Here I focus on a definite group of pairs, namely, close pairs, to investigate the important point, often neglected, that *closeness in the plane of sky is not always a guarantee of three-dimensional closeness*.

An example from our backyard is useful as an illustration. Let us consider the most trivial galaxy pair: the Milky Way-Andromeda system (MW-And). Being the dominant galaxies in the Local Group, these galaxies form a wide pair with 700 kpc of separation. The cartoon in Figure 1 shows the MW-And pair and a line of sight pointing to the outskirts of the Virgo cluster, located at about 15 Mpc. An observer at that location — assuming the Andromeda galaxy with the same linear dimension as the Milky Way galaxy — would notice a difference of less than 5% in their angular size. He could well classify the pair as a close one. With a velocity difference of 119 km s^{-1} at the line-of-sight considered, the MW-And pair would be a strong candidate to be in a list of close pairs. The reality is of another nature: MW-And is a wide pair. Its apogalacticon separation might be estimated at about 2 Mpc, if the system is on a high-eccentric orbit and galaxies have approximately 10^{12} M_\odot . Most plausible, the system has recently reached its apocentric configuration on a low-eccentric orbit, implying a significant transverse velocity at present. The proper motion of M31 has been indeed constrained to about 100 km s^{-1} by Loeb et al. (2005).

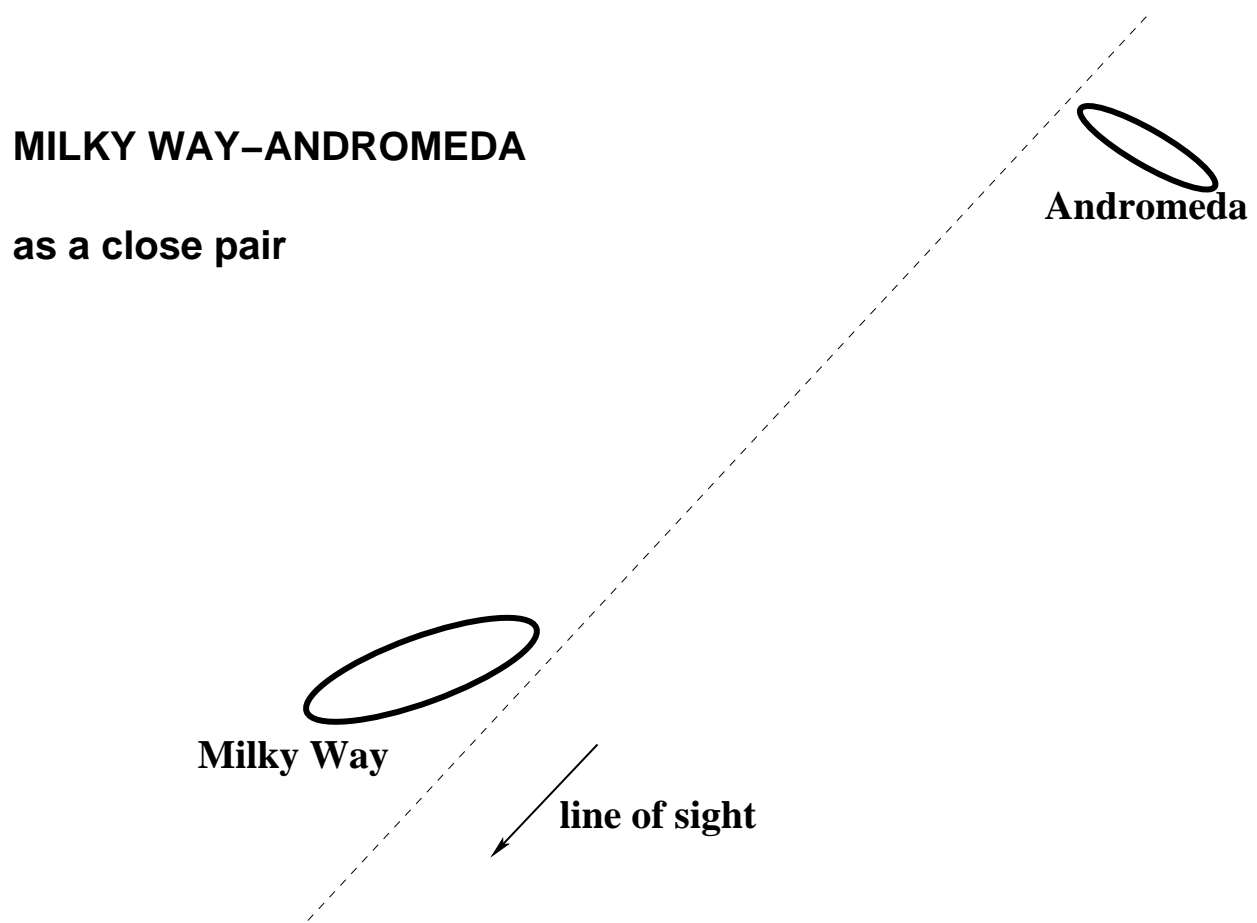


Fig. 1.— The Milky Way-Andromeda system and a line of sight towards a hypothetical distant observer.

Recent papers aiming on the investigation of a number of properties of close pairs, such as star formation (Barton et al. 2000, Woods et al. 2006) and merger rates, do not give due relevance to the fact that projected physical separation (R_p) cannot suffice an unique constraint for closeness. Patton et al. (2000, 2002) define a close pair as having $5\text{h}^{-1} < R_p \leq 20\text{h}^{-1}$ kpc and an upper limit in the pair radial-velocity difference of 500 km s $^{-1}$. The velocity criterion represents a somewhat loose general constraint on physical association. They are followed by others in essentially the same procedure (e.g., Nikolic et al. 2004). I argue here that this is *just* the first step in the selection procedure. It has to be complemented by an investigation of the *tidal* effects on the individual galaxies in the pair in order to have a clear definition of *closeness*.

Other studies address the presence of Markarian activity in galaxy pairs. Byrd & Valtonen (2001) find that Markarian activity is an indication of tidal interaction. Their results should be confronted with the closeness of the sample pairs identified by an *activity-blind* procedure, as suggested here.

In section 2 I show, using Monte Carlo simulations, that small projected separation is not a secure and fair indication of small spatial separation. This is a consequence of the fact that 2-body orbits have most of their phase-space time at apocentric configurations (cf. Kepler's law). The scene is thus set for the presentation of the *classification scheme* in section 3. The relevant observational data for sorting up *apparently* close pairs throughout classes are suggested in section 4.

Section 5 summarizes the main conclusions.

2. Spatial and projected separations in close pairs

The most simple way of disclosing the three-dimensionality of projected separations in binary galaxies is by means of Monte Carlo-type simulations of bound pairs. They are generally an useful tool when one wants to analyze an observed binary sample in order to extract information such as galaxy mass and angular momentum, orbital period and eccentricity, etc. Such a statistical method has been used intensively in the past (e.g., Turner 1976, van Moorsel 1982, Schweizer 1987, Oosterloo 1988, Soares 1990, 1996).

To simulate a sample of binary galaxies a number of input orbital parameters have to be specified, namely, the distribution of spatial separations and of orbital eccentricities. Furthermore, a mass model for galaxies has to be defined and also projection rules to transform orbital velocity and radial separation into observed quantities like line-of-sight velocity difference and apparent projected separation.

2.1. Simulation procedure

The simulation procedure is established according to the objective one has in mind. Here the main goal is to investigate *how close pairs, defined by their apparent separations, are distributed in three dimensions or, in other words, are distributed in the apparent versus spatial separation plane*. The simulations are case problems that span a wide range of possibilities in the whole phase-space of binary orbits. To reach the goal we generated samples of 2000 artificial pairs with the following specifications.

- (i) Mass model: two equal-mass galaxies in Keplerian orbits. Galaxies move under their mutual point-mass Newtonian gravitational potential. We further add the restriction that galaxies never get closer than the sum of their (approximate) half-mass radii. We adopt a conservative value of 10 kpc for the sum. In practice this means that galaxies getting closer than this limiting separation rapidly merge and are therefore excluded from the simulated sample. Self-consistent N-body simulations of binary-galaxy orbit secular evolution have conclusively shown that such systems indeed merge in a time-scale much smaller than a Hubble time (e.g., Bartlett & Charlton 1995, Chan & Junqueira 2001). Evidently galaxies are not point-masses and may possess well-extended (dark) mass distributions. As long as the binary system is isolated from a third-body gravitational influence and furthermore the mutual gravitational interaction is only radial-dependent, the point-mass assumption is a reasonable description of the general consequences of orbital angular momentum conservation, that lays down on the roots of Kepler's areal law, i.e., on the fact that *galaxies spend most of their time at apocenter*.
- (ii) Spatial separation: samples with either a fixed apocentric separation R_{apo} of 200 kpc or 600 kpc. These two values span fairly the average (apocentric) separations of binary galaxies as suggested by several works (Soares 1989, Schweizer 1987, Charlton & Salpeter 1991, Chengalur 1994, Nordgren 1997). A more rigorous simulation should consider a distribution of binary spatial separations. Earlier work (Gott & Turner 1979, but see Soares 1989, chapter 2) suggested that binary galaxies follow, down to small scales, an extension of the classical galaxy two-point correlation function (Peebles 1980), but more recent evidence points to a multi-variable correlation function, depending on galaxy type, luminosity and local galaxy number density. R_{apo} smaller than 200 kpc is not considered here because, as mentioned above, such pairs merge quickly.
- (iii) Eccentricity distribution: three distributions, spanning the entire orbital phase-space. They are $f(e) = \delta(0.9)$, $f(e) = 2e$, and $f(e) = \delta(0)$. If binary galaxies are formed by

early capture, suggested already in 1937 by Holmberg (see also Schweizer 1987), the triangular distribution $f(e) = 2e$ would be suitable since it allows for some amount of transverse orbital motion. The extreme cases of highly eccentric orbits ($e = 0.9$) and circular orbits bracket the triangular distribution and are considered for completeness and shall reveal fruitful consequences (see below).

(iv) Projection on the sky: the normal to the orbital plane is distributed at random *in space*, that is, the orbital inclination i has a distribution $f(i) \propto \sin(i)$.

A pair orbit is simulated with prescriptions (i) through (iii); velocities and radial separations are drawn at a random time instant within the orbit, and from (iv), projected separation onto to the plane of sky and the corresponding line-of-sight pair velocity difference are calculated. The random choice of orbital phase implies, from Kepler’s law, that pairs at apocenter — *large separations* — are naturally favored. For each pair of R_{apo} and $f(e)$ the process is repeated until a list of 2000 pairs is simulated, and therefrom we investigate the correlation between projected and spatial separation.

2.2. Projected versus spatial separation

A *putative* close pair is defined as a pair of galaxies having at most the fiducial projected separation $R_{p,max} = 50$ kpc, which is typical in the studies mentioned above. We then ask: *How many pairs with $R_p \leq R_{p,max}$ have spatial separations $R > R_{p,max}$?*

Figure 2 shows histograms $N - R_p$ for the two cases considered here, $R_{apo} = 200$ and 600 kpc, and for the three distributions of eccentricities, $f(e) = \delta(0.9)$, $f(e) = 2e$ and $f(e) = \delta(0)$. Shaded areas represent close pairs as defined above. Sample median values of R_p are shown in the figure and in Table 1. As expected the least median R_p occurs for $f(e) = \delta(0.9)$ and for the triangular distribution $f(e) = 2e$, being essentially the same for both distributions. It

Table 1: Number of simulated close pairs out of 2000

R_{apo}	$f(e) = \delta(0.9)$	$f(e) = 2e$	$f(e) = \delta(0)$
	Median R_p	Median R_p	Median R_p
200 kpc	284	228	51
	121 kpc	125 kpc	173 kpc
600 kpc	67	30	4
	360 kpc	360 kpc	520 kpc

amounts 60% of R_{apo} , meaning about 120 kpc and 360 kpc respectively. In the simulations of pairs in circular orbits, the median R_p is exactly 87% of R_{apo} . It can be noted from Fig. 2 that the R_p -distributions are the same irrespective of R_{apo} for all eccentricities. Such an overall behavior is expected due to self-similarity, since the dynamical problem is the same with the sole difference on the orbit length-scale. There is a slight fluctuation though in the triangular eccentricity distribution case (middle panels in Fig. 2), which is due to the additional degree of freedom introduced by the random choice of the pair eccentricity. But even here, R_p -distributions are the same, with a noticeable decrease of pairs at small projected separations as compared to the high-eccentricity simulations (top panels).

The important difference between the distributions with $R_{apo} = 200$ kpc and $R_{apo} = 600$ kpc is the percentage of close pairs ($R_p \leq 50$ kpc). According to Table 1, 14% of the total population of pairs with $f(e) = \delta(0.9)$ and $R_{apo} = 200$ kpc are close pairs, a figure that decreases to 3% if $R_{apo} = 600$ kpc. This is a ready consequence of the much wider phase-space available for pairs with the larger R_{apo} .

As seen above, all simulations have large median R_p , even greater than $2 \times R_{p,max}$, which shows that at least half of simulated pairs have *spatial* separations much greater than $R_{p,max}$. This is further confirmed by the data shown in Table 2, which represent the most important result, as far as the classification of close pairs is concerned: *more than half of the simulated pairs with $R_p \leq 50$ kpc have three-dimensional separations greater than 50 kpc*.

If real binaries are predominantly in circular orbits, 100% of pairs have — from input — spatial separation $R > 50$ kpc, and close pairs are thus very few, less than 3% of the simulated population. The firm conclusion from these results is that *apparent separations are not bona-fide indicators of spatial closeness*. Close pairs with $R_{apo} < 200$ kpc, not included in the simulations, would not substantially alter the conclusion.

In the next section, a classification scheme is put forward whose main purpose is to discriminate close pairs against their *real* physical dynamical character. The classification is a pre-requisite for any further astrophysical investigation of the properties of galaxies in close pairs.

Table 2: Percentage of close pairs with $R > 50$ kpc

R_{apo}	$f(e) = \delta(0.9)$	$f(e) = 2e$	$f(e) = \delta(0)$
200 kpc	52.5%	69.3%	100%
600 kpc	53.7%	73.3%	100%

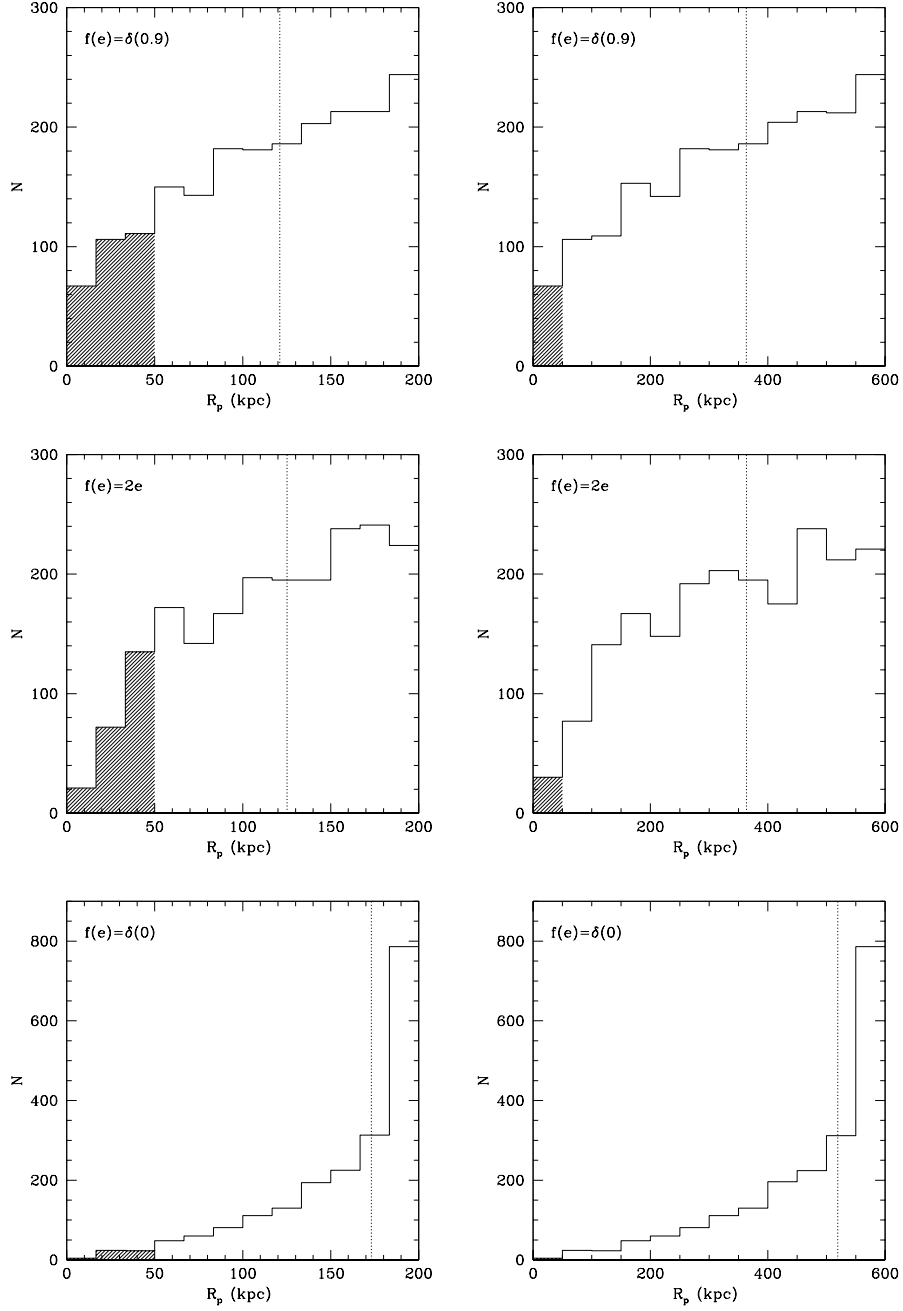


Fig. 2.— Distribution of projected separations R_p for simulated pairs, with different eccentricity distributions $f(e)$ and apocentric separation R_{apo} . Left panels: $R_{apo} = 200$ kpc. Right panels: $R_{apo} = 600$ kpc. Dotted vertical line in all panels marks each sample's median R_p . Shaded areas show the close-pair population.

3. The classification scheme

The ground property in the classification scheme is the *strength of tidal interaction* between pair galaxies. Table 3 shows the four suggested classes of close pairs. The main goal is clearly discriminating between pairs which are interacting through tidal forces and those whose galaxies do not have their internal structure substantially affected by the mutual differential gravitational interaction. The strength of tidal activity between two extended mass distributions, with centers of mass separated by R is — grossly speaking — inversely proportional to R^3 , thus justifying the consideration of tidal activity as the crucial property for a classification scheme. As seen in Table 3, types CP I — mergers — and CP IV — *unphysical* pairs — are extreme types. Type I pairs are evolved type II pairs, and type IV are misclassified close pairs, i.e., optical pairs.

Any study of the effects of closeness on the properties of galaxy pairs must be preceded by an observational selection procedure in order to classify the sample under study into the four classes. In the next section suggestions for the required observational programs are given.

4. Observational strategy for classifying close pairs

4.1. CP I and CP IV

CP I are easily sorted out just looking to their optical disturbed morphology. Individual galaxies are hardly seen as separate entities. CP IV, on the other hand, are selected by their discordant redshifts. A very conservative lower limit to the line-of-sight galaxy velocity difference in the pair of 300 km s^{-1} may be adopted as an initial guess to distinguish optical pairs. This limit corresponds to the relative velocity of two 10^{12} M_\odot (visible plus dark) galaxies on a circular orbit and whose centers of mass are separated by 100 kpc. A detailed study of redshift asymmetries in the pair sample under investigation might be used in order

Table 3: Classification of close pairs

Class	Pair	Interaction
CP I	merger	strongest
CP II	tide-loud	strong
CP III	tide-quiet	weak
CP IV	<i>optical</i>	weakest

to evaluate the contamination by optical companions. Valtonen & Byrd (1986) find that physical pairs exhibit an equal number of positive or negative redshifts relative to the primary while that is not true for non-physical optical pairs.

The most difficult to classify are CP II and CP III requiring a specially suitable observational strategy that takes into account the kinematical consequences of tidal forces.

4.2. Tidal kinematics

A straight application of the *impulse approximation* (Binney & Tremaine 1987) for tidal effects in high-speed encounters (“flybies”) of extended objects, leads to symmetrical perturbations. That is, two test particles, at symmetric positions with respect to the perturbed object center, acquire velocity increments of the same magnitude and opposite direction (Binney & Tremaine, eq. 7-54, p. 438). This will result in *symmetric velocity profiles*. A perturbed disk galaxy would thus exhibit no signature of tidal forces in its rotational profile.

Although the impulse approximation has been successfully shown to be consistent with numerical experiments for mass and energy exchanges between interacting spherical galaxies (Aguilar & White 1985), it does not hold here. Bound pairs are at middle way between the flyby encounters where the impulse approximation does apply and pairs that are quickly evolving through a merger phase. Concerning the latter case, Mihos, Dubinski & Hernquist (1998) made a N-body merger model of NGC 7252, a galaxy with conspicuous tidal tails. The initial pre-merger galaxies have symmetrical rotation curves that evolve along the merger process to a final asymmetrical velocity profile (see their Fig. 6). Hence, one expects that at perigalacticon, bound pairs will show slightly — but noticeable — distorted velocity profiles before they ultimately enter in a merging phase.

Furthermore, Barton et al. (1999) have shown, using N-body simulations of galaxy encounters, that tidal interactions induce noticeable distortions on the rotation curves of spiral galaxy models (see their Fig. 1).

The asymmetry of the velocity profile of both galaxies at closest approach will be used here as an indication of *strong* — loud — tidal forces, implying therefore spatial proximity. This is the rationale under the discussion of the kinematics of CP II and CP III classes below.

4.3. CP II and CP III

The most confident criteria for CP II and CP III classification are: (i) broadband photometry, (ii) kinematics from optical single-slit spectroscopy, and (iii) global HI spectral line low-resolution velocity profiles. These are intentionally designed to be *low cost* procedures for the classification. Strong tidal forces affect the outcome of all three sorts of observations. Ideally, the three should be used, as, for example, in Marziani et al. (1999). They studied the close pair UGC 3995A+B (CPG 140, in Karachentsev 1972, 1987), whose POSS-II B-band image is shown in Fig. 3.

Galaxy centers are separated by approximately $30''$, and the smaller component B is seen in front of the spiral disk of component A. Marziani et al. proceeded to broadband photometry decomposition and found unperturbed individual solutions for both galaxies. Optical spectroscopy reveals symmetrical kinematics relative to the galaxy centers. That is, the rotation curve amplitudes are the same on the receding and approaching sides of both galaxies. The HI global profile is symmetrical as well. The optical velocity difference is 20 km s^{-1} (internal error of 18 km s^{-1}) and the HI velocity difference is 1 km s^{-1} , from Sulentic & Arp (1983). These observations suggest that the pair is a CP III, a *tide-quiet* close pair, seen at or close to apocentric orbital phase, near turnover. It is worthwhile mentioning that the orbital interpretation above diverges from Marziani et al.. They claim that the pair is seen either before or after their closest approach. This seems unlikely though because in this case tidal perturbations would be evident in the observations. The classification scheme relies on the assumption that tidal activity impresses asymmetrical signatures on morphology and kinematics.

A counter-example to UGC 3995, namely, a *tide-loud* close pair, is SBG 249 (Soares et al. 1995). Long-slit spectroscopy has been measured and analyzed by Carvalho & Soares (2007, in preparation). The galaxies are NGC 1738 (eso-lv 5520490) and NGC 1739 (eso-lv 5520500). They have partially overlapped disks. Two spectra were obtained with the Double Spectrograph instrument mounted at the Palomar 5 m telescope, on 1998 February 27-28. Figure 4 shows an isophote map of the pair, with the $128''$ -long slits superposed. The derived rotation curves are shown in Fig. 5 (both figures from Carvalho & Soares 2007, in preparation).

The asymmetry is apparent in NGC 1738 and hinted in NGC 1739. The southwest side of NGC 1738 rotates almost twice as much as the northeast side, that is, its closest side to NGC 1739 rotates at greater speed than the farthest side. The northwest side of NGC 1739 flattens out at about 100 km s^{-1} while the southeast side seems to be rising up at the last measured point. It is clear that the rotation profiles are strongly affected by their mutual tidal influence. On the other hand, the spectrum of the overlapped portion of the system is



Fig. 3.— B-band image from the POSS-II Digital Sky Survey of the close pair UGC 3995A+B. The smaller galaxy B is seen in front of the disk of the larger component. See also Marziani et al. (1999). North is up and east is left.

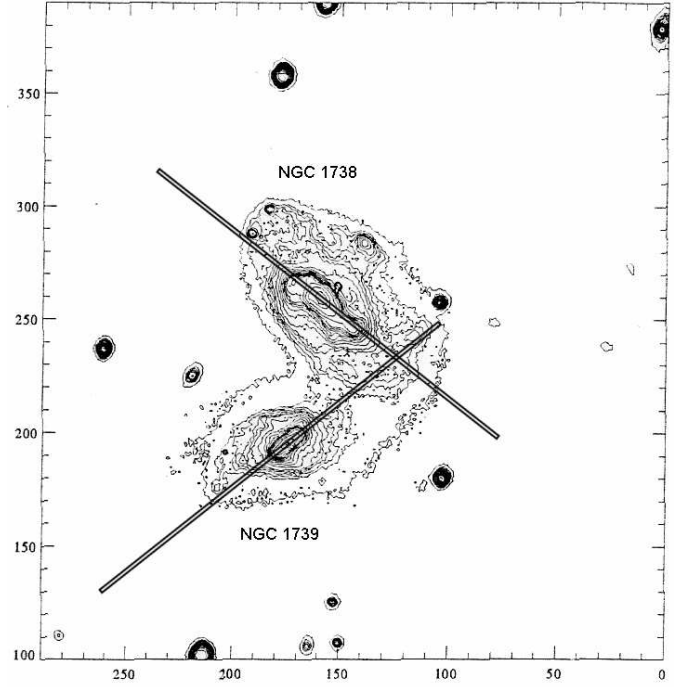


Fig. 4.— R-band isophote map of SBG 249 from Carvalho & Soares (2007, in preparation). NGC 1738 (ESO-LV 552490) is the background galaxy. Slits are $128''$ long. North is up and east left.

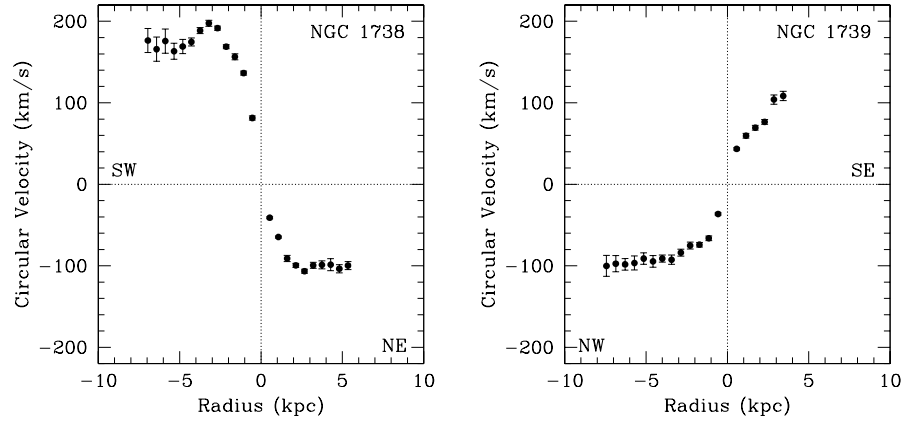


Fig. 5.— Rotation curve of NGC 1738 (left panel) and NGC 1739 (Carvalho & Soares 2007, in preparation). The southwest side (SW) of NGC 1738 disk and the northwest side (NW) of NGC 1739 are partly overlapped.

clearly disentangled showing that both disks rotate quite independently and, as can be seen in Fig. 5, in opposite directions. This also rules out the classification as CP I, in spite of the pair disturbed morphological appearance.

The line-of-sight velocity difference is 60 km s^{-1} (internal error of 20 km s^{-1}). Since they are low-mass galaxies, this is consistent with SBG 249 being a CP II seen at or close to perigalacticon in an eccentric orbit (cf. appendix in Soares 1996). Additional broadband photometry and global HI observation are planned for the pair.

The strength of the asymmetry in the velocity profile might depend on the disk rotation sense relative to the orbit sense. Howard et al. (1993) performed detailed simulations of tidally induced structures in disk galaxies. They discuss morphological disturbances and find that retrograde encounters are less effective in producing disturbances. If the result applies also to kinematical disturbances then pairs that pass close enough to be CP II — tide-loud pairs — might resemble CP III types if the galaxy’s rotation sense is opposite to the orbit sense. These cases require careful analysis of *both* broadband photometry and pair kinematics as was the case of CPG 140 discussed above.

5. Conclusion

Monte Carlo simulations of close pairs of galaxies show that projected separation restrictive criterion does not guarantee closeness in space. Accordingly, a simple classification scheme of close pairs is proposed and an observational strategy is suggested for sorting out a sample before any kind of astrophysical investigation of their properties is made. The classification is based on kinematical and dynamical criteria and on the pair overall morphological appearance. The required observations are thus broadband photometry, optical and HI 21-cm line spectroscopy. The latter is of course only suitable for pairs with late-type galaxies.

For a sample of close pairs, defined initially by their closeness in the plane of sky, the three kinds of observations are sufficient in ascribing to each pair one of the classes suggested. Classes are defined by the strength of present tidal activity and optical morphology. They are: mergers (CP I), tide-loud pairs (CP II), tide-quiet pairs (CP III) and physically unbound *optical* pairs (CP IV).

I thank David Balparda de Carvalho for helpful discussions on the close-pair subject and for a careful reading of the manuscript. The anonymous referee is gratefully acknowledged for useful comments and suggestions to improve the text. The Second Palomar Observatory

Sky Survey (POSS-II) was made by the California Institute of Technology with funds from the National Science Foundation, the National Geographic Society, the Sloan Foundation, the Samuel Oschin Foundation, and the Eastman Kodak Corporation.

REFERENCES

Aguilar, L.A., & White, S.D.M. 1985, *ApJ*, 295, 374

Bartlett, R.E., & Charlton, J.C. 1995, *ApJ*, 449, 447

Barton, E.J., Bromley, B.C., & Geller, M.J., 1999, *ApJ*, 511, L25

Barton, E.J., Geller, M.J., & Kenyon, S.J., 2000, *ApJ*, 530, 660

Binney, J., & Tremaine, S. 1987, *Galactic Dynamics*, (Princeton: Princeton University Press)

Byrd, G., & Valtonen, M.J. 2001, *AJ*, 121, 2943

Chan, R., & Junqueira, S. 2001, *A&A*, 366, 418

Charlton, J.C., & Salpeter, E.E. 1991, *ApJ*, 375, 517

Chengalur, J.N. 1994, PhD thesis, Cornell University

Chengalur, J.N., Salpeter, E.E., & Terzian, Y. 1993, *ApJ*, 419, 30

Goth, J.R., & Turner, E.L. 1979, *ApJ*, 232, L79

Holmberg, E. 1937, *Annals Obs. Lund*, 6, 1

Howard, S., Keel, W.C., Byrd, G., & Burkey, J. 1993, *ApJ*, 417, 502

Karachentsev, I. 1972, *Soob. Sp. Astr. Obs. Akad. Nauk.*, 7

Karachentsev, I. 1987, *Double Galaxies* (Moscow: Nauka), in Russian

Loeb, A., Reid, M.J., Brunthaler, A., & Falcke, H. 2005, *ApJ*, 633, 894

Marziani, P., D'Onofrio, M., Dultzin-Hacyan, D., & Sulentic, J.W. 1999, *AJ*, 117, 2736

Mihos, J.C., Dubinski, J., & Hernquist, L. 1998, *ApJ*, 494, 183

van Moorsel, G.A. 1982, PhD thesis, University of Groningen

Nordgren, T.E. 1997, PhD thesis, Cornell University

Nordgren, T.E., Chengalur, J.N., Salpeter, E.E., & Terzian, Y. 1993, ApJS, 115, 43

Nikolic, B., Cullen, H., & Alexander, P. 2004, MNRAS, 355, 874

Oosterloo, T.A. 1988, PhD thesis, University of Groningen

Page, T., Dahn, C.C., & Morrison, F.F. 1961, AJ, 66, 614

Patton, D.R., Carlberg, R.G., Marzke, R.O., et al. 2000, ApJ, 536, 153

Patton, D.R., Pritchett, C.J., Carlberg, R.G., et al. 2002, ApJ, 565, 208

Peebles, P.J.E. 1980, The Large-Scale Structure of the Universe (Princeton: Princeton University Press)

Schweizer, L.Y. 1987, ApJS, 64, 427

Soares, D.S.L. 1989, PhD thesis, University of Groningen

Soares, D.S.L. 1990, A&A, 238, 50

Soares D.S.L., de Souza R.E., de Carvalho R.R., & Couto da Silva T.C. 1995, A&AS, 110, 371

Soares, D.S.L. 1996, A&A, 313, 347

Sulentic, J.W., & Arp, H. 1983, AJ, 89, 489

Turner, E.L. 1976, ApJ, 208, 304

Valtonen, M.J., & Byrd, G.G. 1986, ApJ, 303, 523

Woods, D.F., Geller, M.J., & Barton, E.J., 2006, AJ, 132, 197